Remote Tracking Control of Unicycle Robots with Network-Induced Delays

Alejandro Alvarez-Aguirre[1], Nathan van de Wouw[1], Toshiki Oguchi[2], Kotaro Kojima[2], and Henk Nijmeijer[1]

[1] Eindhoven University of Technology, Department of Mechanical Engineering
P.O. Box 513, 5600 MB Eindhoven, The Netherlands
{a.a.alvarez,n.v.d.wouw,h.nijmeijer}@tue.nl
[2] Tokyo Metropolitan University, Department of Mechanical Engineering
1-1, Minami-osawa, Hachioji-shi, Tokyo 192-0397, Japan
t.oguchi@tmu.ac.jp, kojima-koutarou@ed.tmu.ac.jp

Abstract. In this chapter, the tracking control problem for a unicycle-type mobile robot with network-induced delays is addressed. The time-delay affects the system due to the fact that the controller and the robot are linked via a delay-inducing communication channel, by which the performance and stability of the system are possibly compromised. In order to tackle the problem, a state estimator with a predictor-like structure is proposed. Acting in conjunction with a tracking control law, the resulting control strategy is capable of stabilizing the system and compensates for the negative effects of the time-delay. The local uniform asymptotic stability of the closed-loop system is guaranteed up to a maximum admissible time-delay, for which explicit expressions are provided in terms of the system's control parameters. The applicability of the proposed estimator-control strategy is demonstrated by means of experiments carried out between multi-robot platforms located in Eindhoven, The Netherlands and Tokyo, Japan.

Keywords: Mobile robot, Remote tracking control, Network delay, Nonlinear estimator, Non-holonomic systems.

1 Introduction

In the increasingly fast and diverse technological developments of the last decades the duties and tasks conferred to control systems have become much more complex and decisive. Requirements now encompass flexibility, robustness, ubiquity and transparency, among others.

Specifically, the study of robotic systems controlled over a network has become significatively important as a way to support the design of robotic systems that can perform remote, dangerous or distributed tasks. The remote control, or the control of a system subject to a network-induced delay is important in e.g. teleoperation strategies and is a central topic in Networked Control Systems (NCS).

Several techniques have been proposed so far in order to cope with network-induced delays in these settings; e.g. the use of scattering transformations, wave variables formulation, queuing methodologies, delay compensation techniques and robust control

J.A. Cetto et al. (Eds.): Informatics in Control, Automation and Robotics, LNEE 89, pp. 225–238.
springerlink.com

design to name a few. A detailed description of such techniques and many others, together with further references, can be found in e.g. [4], [5], [19].

In this work, a control strategy for the remote tracking control of a unicycle-type mobile robot is proposed. The network-induced delay is compensated by means of a state estimator inspired by the predictor based on synchronization presented in [12], [13]. The main idea behind the state estimator is to reproduce the system's behavior without delay in order to drive an anticipating controller. The problem presents various challenges since the system is nonlinear and subject to a non-holonomic constraint. Additionally, the difficulties faced when implementing the proposed ideas in an experimental setting using the Internet as the communication channel should be taken into account and are also discussed in depth. In [8], a similar state estimator has been applied to a mobile robot subject to a communication delay, and sufficient conditions for the estimator's convergence have been derived. In this work an alternative approach is taken in order to prove the stability of the entire closed-loop system consisting of the mobile robot, the tracking controller and the state estimator.

This chapter is structured in the following way. Section 2 recalls results on the tracking control of a delay-free unicycle-type mobile robot. In Section 3 a control scheme intended to control a mobile robot with a network-induced time-delay is proposed and conditions on the maximum allowable time-delay in terms of the control parameters are posed. Section 4 provides an overview of the experimental platform used to validate the control strategy proposed, explains how the most critical implementation issues have been addressed, and presents the experimental results. Finally, conclusions are provided in Section 5.

2 Tracking Control of a Unicycle Robot

The tracking control design for a unicycle-type mobile robot is discussed in this section. To begin with, consider the posture kinematic model of a unicycle:

$$\begin{aligned} \dot{x}(t) &= v(t)\cos\theta(t), \\ \dot{y}(t) &= v(t)\sin\theta(t), \\ \dot{\theta}(t) &= \omega(t), \end{aligned} \tag{1}$$

in which $x(t)$ and $y(t)$ denote the robot's position in the global coordinate frame X-Y (cf. Figure 1), $\theta(t)$ defines its orientation with respect to the X-axis, and $v(t)$ and $\omega(t)$ constitute the robot's translational and rotational velocities, respectively, and are regarded as the system's control inputs. The robot's state is defined by $q(t) = [x(t)\ y(t)\ \theta(t)]^T$ and the non-slip condition on the unicycle's wheels imposes a non-holonomic constraint on the system, as explained in [1].

The control objective is to track a time-varying reference trajectory specified by $q_r(t) = [x_r(t)\ y_r(t)\ \theta_r(t)]^T$. The reference position $(x_r(t), y_r(t))$ satisfies the dynamics,

$$\begin{aligned} \dot{x}_r(t) &= v_r(t)\cos\theta_r(t), \\ \dot{y}_r(t) &= v_r(t)\sin\theta_r(t), \end{aligned} \tag{2}$$

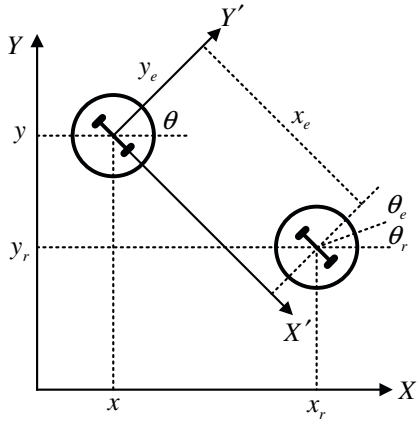

Fig. 1. Mobile robot, reference system, and error coordinates.

while the reference orientation $\theta_r(t)$, translational velocity $v_r(t)$, and rotational velocity $\omega_r(t)$ are defined in terms of the reference Cartesian velocities $\dot{x}_r(t)$, $\dot{y}_r(t)$ and accelerations $\ddot{x}_r(t)$, $\ddot{y}_r(t)$ as follows:

$$\theta_r(t) = \text{arctan2}\left(\dot{y}_r(t), \dot{x}_r(t)\right), \tag{3}$$

$$v_r(t) = \sqrt{\dot{x}_r^2(t) + \dot{y}_r^2(t)}, \tag{4}$$

$$\omega_r(t) = \frac{\dot{x}_r(t)\ddot{y}_r(t) - \ddot{x}_r(t)\dot{y}_r(t)}{\dot{x}_r^2(t) + \dot{y}_r^2(t)} = \dot{\theta}_r(t), \tag{5}$$

where atan2 is the arctangent function of two arguments. It is worth noting that computing (3) and (5) requires either $\dot{x}_r(t) \neq 0$ or $\dot{y}_r(t) \neq 0$ at all times.

The difference between the reference trajectory and the state evolution may be expressed with respect to the system's local coordinate frame X'-Y' in order to define the error coordinates $q_e(t) = [x_e(t)\ y_e(t)\ \theta_e(t)]^T$, as proposed by [7] and shown in Figure 1. These tracking error coordinates are given by,

$$\begin{bmatrix} x_e(t) \\ y_e(t) \\ \theta_e(t) \end{bmatrix} = \begin{bmatrix} \cos\theta(t) & \sin\theta(t) & 0 \\ -\sin\theta(t) & \cos\theta(t) & 0 \\ 0 & 0 & 1 \end{bmatrix} \begin{bmatrix} x_r(t) - x(t) \\ y_r(t) - y(t) \\ \theta_r(t) - \theta(t) \end{bmatrix}. \tag{6}$$

Exploiting (1), (2), (5), and (6), the tacking error dynamics result in,

$$\begin{aligned} \dot{x}_e(t) &= \omega(t)y_e(t) + v_r(t)\cos\theta_e(t) - v(t), \\ \dot{y}_e(t) &= -\omega(t)x_e(t) + v_r(t)\sin\theta_e(t), \\ \dot{\theta}_e(t) &= \omega_r(t) - \omega(t). \end{aligned} \tag{7}$$

The following tracking controller has been proposed in [6], [15],

$$\begin{aligned} v(t) &= v_r(t) + c_2 x_e(t) - c_3\omega_r(t)y_e(t), \\ \omega(t) &= \omega_r(t) + c_1 \sin\theta_e(t), \end{aligned} \tag{8}$$

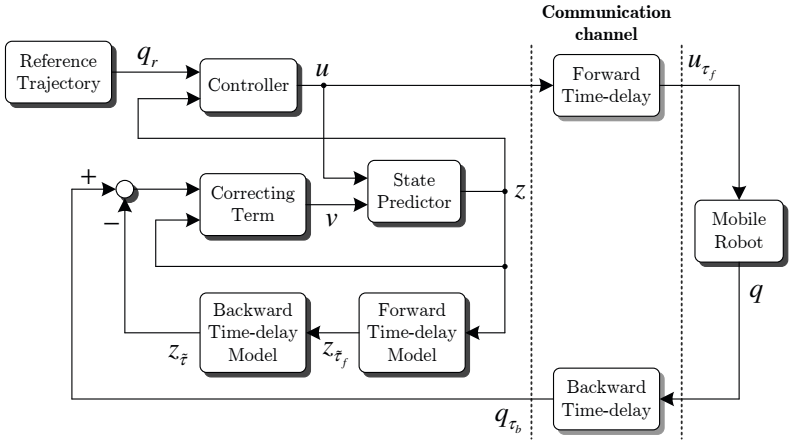

Fig. 2. Block diagram representation of proposed remote tracking control strategy.

which ensures local exponential stability (LES) of the tracking error dynamics (7)-(8) if $c_1, c_2 > 0$ and $c_3 > -1$.

3 Remote Tracking Control

In this section, we consider a mobile robot controlled over a network which induces time-delays, see Figure 2. The robot's controller, consisting of the tracking control law (8) and a state estimator, should ensure that the robot tracks (a delayed version) of the reference trajectory. The state estimator has a predictor-like structure and is similar to the one proposed in [8]. The origin of this type of predictor can be traced back to the appearance of the notion of anticipating synchronization in coupled chaotic systems, which was first noted by [20]. After the same behavior was observed in certain simple physical systems such as specific electronic circuits and lasers, it was studied for more general systems in [14]. As a result of this generalization, a state predictor based on synchronization for nonlinear systems with input time-delay was proposed in [12]. The same concept, which can be seen as a state estimator with a predictor-like structure, is proposed here for a mobile robot subject to a network-induced delay.

3.1 State Estimator and Controller Design

When considering a network-induced delay, the mobile robot is subject not only to a forward τ_f (input) time-delay, but also to a backward τ_b (output) time-delay, as denoted in [5]. Hereinafter the forward and backward time-delays τ_f, τ_b will be assumed to be constant and known, with $\tau := \tau_b + \tau_f$. Given the mobile robot (1) subject to a network-induced input delay τ_f, the robot's posture kinematic model is given by,

$$\begin{aligned} \dot{x}(t) &= v(t-\tau_f)\cos\theta(t), \\ \dot{y}(t) &= v(t-\tau_f)\sin\theta(t), \\ \dot{\theta}(t) &= \omega(t-\tau_f). \end{aligned} \tag{9}$$

Moreover, the system's state measurements are affected by a backward time-delay τ_b: $q(t-\tau_b) = [x(t-\tau_b)\ y(t-\tau_b)\ \theta(t-\tau_b)]^T$.

In order to improve the tracking performance when subject to a communication delay, the following state estimator, with state $z(t) = [z_1(t)\ z_2(t)\ z_3(t)]^T$, is proposed:

$$\begin{aligned} \dot{z}_1(t) &= v(t)\cos z_3(t) + \nu_x(t), \\ \dot{z}_2(t) &= v(t)\sin z_3(t) + \nu_y(t), \\ \dot{z}_3(t) &= \omega(t) + \nu_\theta(t), \end{aligned} \tag{10}$$

with $\nu(t) = [\nu_x(t)\ \nu_y(t)\ \nu_\theta(t)]^T$ defining a correcting term based on the difference between the estimator state and the measured state.

For the purpose of designing the correcting term $\nu(t)$, two new sets of error coordinates are introduced, namely $z_e(t)$ and $p_e(t)$. The first set of error coordinates relates to the difference between the estimator state $z(t)$ and the reference trajectory $q_r(t)$:

$$\begin{bmatrix} z_{1_e}(t) \\ z_{2_e}(t) \\ z_{3_e}(t) \end{bmatrix} = \begin{bmatrix} \cos z_3(t) & \sin z_3(t) & 0 \\ -\sin z_3(t) & \cos z_3(t) & 0 \\ 0 & 0 & 1 \end{bmatrix} \begin{bmatrix} x_r(t) - z_1(t) \\ y_r(t) - z_2(t) \\ \theta_r(t) - z_3(t) \end{bmatrix}. \tag{11}$$

The second set of error coordinates relates to the difference between the delayed estimator state $z(t-\tilde{\tau})$ and the delayed system state $q(t-\tau_b)$:

$$\begin{bmatrix} p_{1_e}(t) \\ p_{2_e}(t) \\ p_{3_e}(t) \end{bmatrix} = \begin{bmatrix} \cos z_3(t-\tilde{\tau}) & \sin z_3(t-\tilde{\tau}) & 0 \\ -\sin z_3(t-\tilde{\tau}) & \cos z_3(t-\tilde{\tau}) & 0 \\ 0 & 0 & 1 \end{bmatrix} \begin{bmatrix} x(t-\tau_b) - z_1(t-\tilde{\tau}) \\ y(t-\tau_b) - z_2(t-\tilde{\tau}) \\ \theta(t-\tau_b) - z_3(t-\tilde{\tau}) \end{bmatrix}, \tag{12}$$

where $\tilde{\tau} := \tilde{\tau}_f + \tilde{\tau}_b$ represents the sum of the modeled forward and backward network-induced delays. Recall that the time-delays are assumed to be known or, in other words, modeled perfectly, i.e. $\tilde{\tau}_f = \tau_f$ and $\tilde{\tau}_b = \tau_b$, which yields $\tilde{\tau} = \tau$.

Given the error coordinates (12), the correcting term $\nu(t)$ is proposed as follows:

$$\begin{aligned} \nu_x(t) &= -K_x p_{1_e}(t)\cos z_3(t) + K_y p_{2_e}(t)\sin z_3(t), \\ \nu_y(t) &= -K_x p_{1_e}(t)\sin z_3(t) - K_y p_{2_e}(t)\cos z_3(t), \\ \nu_\theta(t) &= -K_\theta \sin p_{3_e}(t), \end{aligned} \tag{13}$$

where K_x, K_y and K_θ are the correcting term gains.

The block diagram representation of the proposed control scheme is depicted in Figure 2, and shows that the state estimator's output constitutes the controller's input. The tracking control law (8) will now make use of the estimated error coordinates (11) and will be given by,

$$\begin{aligned} v(t) &= v_r(t) + c_2 z_{1_e}(t) - c_3\omega_r(t) z_{2_e}(t), \\ \omega(t) &= \omega_r(t) + c_1 \sin z_{3_e}(t). \end{aligned} \tag{14}$$

Remark 1. Due to the input time-delay τ_f, the control action applied to the robot in (9) is given by:

$$\begin{aligned} v(t-\tau_f) &= v_r(t-\tau_f) + c_2 z_{1_e}(t-\tau_f) - c_3\omega_r(t-\tau_f) z_{2_e}(t-\tau_f), \\ \omega(t-\tau_f) &= \omega_r(t-\tau_f) + c_1 \sin z_{3_e}(t-\tau_f). \end{aligned}$$

The resulting control action already hints at how we would like the system to behave. Intuitively, the robot state $q(t)$ should track the delayed reference trajectory $q_r(t-\tau_f)$. This will be examined in detail during the stability analysis in Section 3.2.

3.2 Stability Analysis

The control objectives may now be defined as follows:

- $q(t) \to q_r(t-\tau_f)$, the system states converge to the reference trajectory delayed by τ_f;
- $z(t) \to q(t+\tau_f)$, the state estimator anticipates the system by τ_f;
- $z(t) \to q_r(t)$, the state estimator converges to the reference trajectory.

Considering these control objectives and taking into account Remark 1, the following control goal can now be formulated:

Given the unicycle-type mobile robot (9) subject to a network induced delay $\tau = \tau_f + \tau_b$, the state estimator (10), (12)-(13), and the control law (11), (14), the robot should track a delayed version $q_r(t-\tau_f)$ of the reference trajectory.

In order to meet this control goal we aim to prove the stability of the equilibrium point $(z_e, p_e) = (z_{1_e}, z_{2_e}, z_{3_e}, p_{1_e}, p_{2_e}, p_{3_e}) = 0$ of the closed-loop system (9)-(14).

Consider the following error coordinate definitions: $\xi_1 = [z_{1_e}\ z_{2_e}\ p_{1_e}\ p_{2_e}]^T$ and $\xi_2 = [z_{3_e}\ p_{3_e}]^T$, with z_{i_e}, p_{i_e}, $i = 1, 2, 3$, defined in (11) and (12), respectively. Using these definitions, the resulting closed-loop error dynamics can be rearranged in the following form:

$$\dot{\xi}_1(t) = A_1(t, t-\tau)\xi_1(t) + A_2\xi_1(t-\tau) + g(t, \xi_{1_t}, \xi_{2_t}), \tag{15}$$

$$\dot{\xi}_2(t) = f_2(t, \xi_{2_t}), \tag{16}$$

where ξ_{i_t}, $i = 1, 2$, is an element of the Banach space $C(n) = C([-\tau, 0], R^n)$ and is defined by the formula $\xi_{i_t}(s) = \xi_{i_t}(t+s)$ for $s \in [-\tau, 0]$. By means of ξ_{i_t} it is possible to represent a state ξ_i of the system throughout the interval $t \in [t-\tau, t]$.

The matrices and functions defining the right-hand side in (15)-(16) are given by

$$A_1(t, t-\tau) = \begin{bmatrix} -c_2 & (1+c_3)\omega_r(t) & K_x & 0 \\ -\omega_r(t) & 0 & 0 & K_y \\ 0 & 0 & 0 & \omega_r(t-\tau) \\ 0 & 0 & -\omega_r(t-\tau) & 0 \end{bmatrix}, A_2 = \begin{bmatrix} 0 & 0 & 0 & 0 \\ 0 & 0 & 0 & 0 \\ 0 & 0 & K_x & 0 \\ 0 & 0 & 0 & K_y \end{bmatrix},$$

$$g(t, \xi_{1_t}, \xi_{2_t}) = \begin{bmatrix} g_{11} & g_{12} \\ g_{21} & g_{22} \\ 0 & g_{32} \\ 0 & g_{42} \end{bmatrix} \xi_2(t) + \begin{bmatrix} 0 & 0 \\ 0 & 0 \\ h_{31} & h_{32} \\ h_{41} & h_{42} \end{bmatrix} \xi_2(t-\tau),$$

$$f_2(t, \xi_{2_t}) = \begin{bmatrix} -c_1 \sin z_{3_e}(t) + K_\theta \sin p_{3_e}(t) \\ K_\theta \sin p_{3_e}(t-\tau) \end{bmatrix}, \tag{17}$$

with

$$g_{11} = c_1 z_{2_e}(t) \int_0^1 \cos(s z_{3_e}(t)) ds - v_r(t) \int_0^1 \sin(s z_{3_e}(t)) ds,$$

$$g_{12} = -K_\theta z_{2_e}(t) \int_0^1 \cos(s p_{3_e}(t)) ds,$$

$$g_{21} = (v_r(t) - c_1 z_{1_e}(t)) \int_0^1 \cos(s z_{3_e}(t)) ds,$$

$$g_{22} = K_\theta z_{1_e}(t) \int_0^1 \cos(s p_{3_e}(t)) ds,$$

$$g_{32} = -(v_r(t-\tau) + c_2 z_{1_e}(t-\tau) - c_3 \omega_r(t-\tau) z_{2_e}(t-\tau)) \int_0^1 \sin(s p_{3_e}(t)) ds,$$

$$g_{42} = (v_r(t-\tau) + c_2 z_{1_e}(t-\tau) - c_3 \omega_r(t-\tau) z_{2_e}(t-\tau)) \int_0^1 \cos(s p_{3_e}(t)) ds,$$

$$h_{31} = c_1 p_{2_e}(t) \int_0^1 \cos(s z_{3_e}(t-\tau)) ds,$$

$$h_{32} = -K_\theta p_{2_e}(t) \int_0^1 \cos(s p_{3_e}(t-\tau)) ds,$$

$$h_{41} = -c_1 p_{1_e}(t) \int_0^1 \cos(s z_{3_e}(t-\tau)) ds,$$

$$h_{42} = K_\theta p_{1_e}(t) \int_0^1 \cos(s p_{3_e}(t-\tau)) ds.$$

The definition of a persistently exciting (PE) signal will be required in order to formulate a stability result for the system (15)-(17).

Definition 1. *A continuous function $\omega : \mathbb{R}^+ \to \mathbb{R}$ is said to be persistently exciting (PE) if $\omega(t)$ is bounded, Lipschitz, and constants $\delta_c > 0$ and $\epsilon > 0$ exist such that,*

$$\forall t \geq 0,\ \exists s :\ t - \delta_c \leq s \leq t \text{ such that } |\omega(s)| \geq \epsilon.$$

The following theorem formulates sufficient conditions under which $(z_e, p_e) = 0$ is a locally uniformly asymptotically stable equilibrium point of (15)-(17).

Theorem 1. *Consider the posture kinematic model of a unicycle-type mobile robot subject to a constant and known input time-delay τ_f, as given by (9). The robot's reference position is given by $(x_r(t), y_r(t))$, whereas its reference orientation $\theta_r(t)$ is given by (3). Additionally, consider the tracking controller as given in (14), with the feedforward terms $v_r(t)$ and $\omega_r(t)$ defined in (4) and (5), respectively, and the feedback part based on the error between the reference trajectory and an estimate of the state, as given in (11). Moreover, consider the state estimator (10), (12)-(13), which uses state measurements delayed by a constant and known output time-delay τ_b. If the following conditions are satisfied:*

- *$\omega_r(t)$ is bounded and persistently exciting;*
- *the tracking gains satisfy $c_1, c_2 > 0$, $c_3 > -1$;*
- *the correcting term gains satisfy $K_x = K_y = K < 0$, $K_\theta < 0$;*
- *the time-delay $\tau = \tau_b + \tau_f$ belongs to the interval $0 \leq \tau < \tau_{\max}$, with*

$$\tau_{\max} = \min\left\{\frac{-1}{\sqrt{p}K_\theta}, \frac{-1}{\sqrt{p}(K - \bar{\omega}_r)}\right\}, \tag{18}$$

where $p > 1$ and $\bar{\omega}_r = \sup_{t\in\mathbb{R}} |\omega_r(t)|$,

then, $(z_e, p_e) = 0$ is a locally uniformly asymptotically stable equilibrium point of the closed-loop error dynamics (15)-(17). In other words, $z(t) \to q(t + \tau_f)$ as $t \to \infty$ (the state estimator anticipates the state by τ_f) and $q(t) \to q_r(t - \tau_f)$ as $t \to \infty$ (the system tracks the reference trajectory delayed by τ_f).

Proof. For brevity only a sketch of the proof is presented. Recall the closed-loop error dynamics (15)-(17) and note that systems (15)-(16) form a cascade consisting of a nonlinear delayed system $\dot{\xi}_2(t) = f_2(t, \xi_{2_t})$, interconnected to a linear time-varying delayed system $\dot{\xi}_1(t) = A_1(t, t-\tau)\xi_1(t) + A_2\xi_1(t-\tau)$ by means of a nonlinear delayed coupling $g(t, \xi_{1_t}, \xi_{2_t})$.

Based on Theorem 2 in [18], local uniform asymptotic stability of the equilibrium point $(z_e, p_e) = 0$ of the predictor's closed-loop error dynamics may be established if the following conditions are satisfied,

- the coupling term $g(t, \xi_{1_t}, \xi_{2_t})$ vanishes when $\xi_{2_t} \to 0$, i.e. $g(t, \xi_{1_t}, 0) = 0$;
- the unperturbed subsystem $\dot{\xi}_1(t) = A_1(t, t-\tau)\xi_1(t) + A_2\xi_1(t-\tau)$ is uniformly asymptotically stable;
- subsystem $\dot{\xi}_2(t) = f_2(t, \xi_{2_t})$ is locally uniformly asymptotically stable.

Let us now check the validity of these three conditions. Firstly, given $g(t, \xi_{1_t}, \xi_{2_t})$ as defined in (17), it immediately follows that as $\xi_{2_t} \to 0$, the coupling term vanishes and thus the first condition is satisfied.

Regarding the second condition, subsystem $\dot{\xi}_1(t) = A_1(t, t-\tau)\xi_1(t) + A_2\xi_1(t-\tau)$ can be represented by a cascade itself. Using a similar reasoning as for the original cascade (15)-(17), the subsystem's uniform asymptotic stability is concluded if the time-delay satisfies the following condition:

$$\tau < \frac{-1}{\sqrt{p}(K - \bar{\omega}_r)}, \tag{19}$$

and the requirements for c_2, c_3, K_x and K_y stated in Theorem 1 are satisfied.

In order to check the third condition, subsystem $\dot{\xi}_2(t)$ is first linearized around the equilibrium point $z_{3_e} = p_{3_e} = 0$. The uniform asymptotic stability of the linearized subsystem is ensured for

$$\tau < \frac{-1}{\sqrt{p}K_\theta}, \tag{20}$$

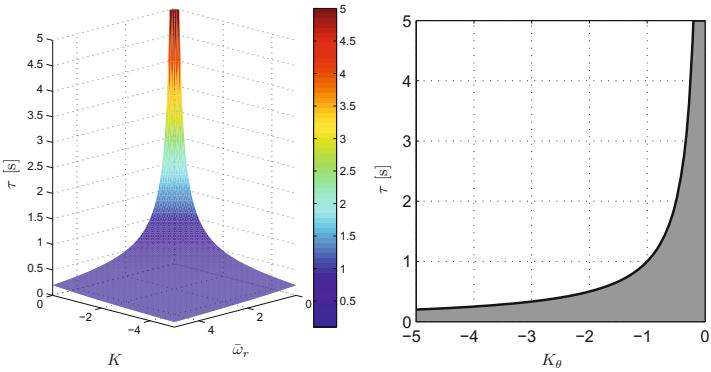

Fig. 3. Maximum allowable time-delay τ for conditions (19) (left) and (20) (right), respectively. To better illustrate the relationship between the gains and the time-delay, the maximum allowable delay in the plot has been cut off at 10 s.

provided c_1 and K_θ satisfy the conditions in Theorem 1. Note that the satisfaction of (19) and (20) is guaranteed by satisfying condition (18) in the theorem.

The local uniform asymptotic stability of the equilibrium point $(z_e, p_e) = 0$ of the closed-loop error dynamics (15)-(17) is then concluded. This means that the state estimator converges to the reference trajectory, since $z_e(t) \to 0$ as $t \to \infty$, or in other words, $z(t) \to q_r(t)$ as $t \to \infty$. It also implies that the state estimator anticipates the system, due to the fact that $p_e(t) \to 0$ as $t \to \infty$, i.e. $z(t) \to q(t + \tau_f)$ as $t \to \infty$. From the previous relations it directly follows that $q(t) \to q_r(t - \tau_f)$ as $t \to \infty$, which means that the unicycle-type mobile robot, subject to a network-induced delay τ, tracks the reference trajectory delayed by τ_f. This completes the sketch of the proof.

The relationship between the allowable time-delay τ and the control parameters for conditions (19) and (20) is shown in Figure 3. The left plot shows the maximum allowable time-delay satisfying (19) considering $p = 1$ and different values for the correcting term gain K and for the maximum reference rotational velocity $\bar{\omega}_r$. Depicted in the right plot is the maximum allowable time-delay satisfying (20) given $p = 1$ and different values for the correcting term gain K_θ. Note that, for both conditions, there exist choices for the correcting term gains such that it becomes possible to accommodate arbitrarily large time-delays ($K \to 0$ and $\bar{\omega}_r \to 0$ for (19) and $K_\theta \to 0$ for (20)). A word of caution is in order, however, since the plots also show that there is a performance tradeoff arising from the relationship between the allowable time-delay, the correcting term gains and the tracking behavior. Namely, decreasing the correcting term gains allows higher robustness for delays at the expense of slower convergence.

4 Experimental Results

Two equivalent multi-robot platforms have been developed at the Eindhoven University of Technology (TU/e), The Netherlands, and at the Tokyo Metropolitan University (TMU), Japan. The proposed remote tracking controller is implemented in such a way that a mobile robot located at TU/e is controlled from TMU and viceversa.

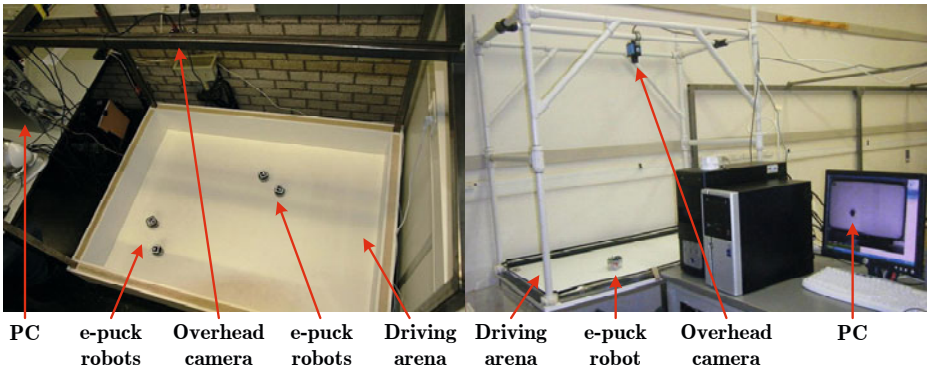

Fig. 4. Experimental setups at TU/e (left) and TMU (right).

4.1 Experimental Platform Description

The experimental platforms' design objectives encompass cost, reliability and flexibility. The corresponding hardware and software choices, together with the implementation of the setup at TU/e are discussed in greater detail in [2], [3] (cf. Figure 4). The setup has already been used to implement cooperation, coordination, collision avoidance and servo vision algorithms, see e.g. [10], [9]. The platform at TMU has similar characteristics, only differing from the one at TU/e in size and in the vision calibration algorithm used. Listed below are some of the experimental platforms' components and characteristics:

- **Mobile Robot.** The unicycle selected is the e-puck mobile robot [11], whose wheels are driven by stepper motors that receive velocity control commands over a BlueTooth connection.
- **Vision.** Each robot is fitted with a fiducial marker of 7 by 7 cm, collected by an industrial FireWire camera, interpreted in the program reacTIVision [17], and calibrated by means of a global transformation (TU/e) or a grid (TMU).
- **Driving Area.** The driving area is of 175×128 cm for TU/e and 100×50 cm for TMU, and is determined based on the required accuracy, the camera lens, and the height at which the camera is positioned.
- **Software.** The e-puck robots and reacTIVision's data stream can be managed in Matlab script, C, or Python. In this work, the controller implementation and signal processing is carried out in Python [16].
- **Bandwidth and Sampling Rate.** Using vision as the localization technique diminishes the system's bandwidth and results in a sampling rate of 25 Hz.

4.2 Data Exchange over the Internet

Due to its widespread availability and low cost, the Internet is chosen as the communication channel to exchange data between TU/e and TMU. Details about the data exchange implementation are given below:

- **Data Exchange.** A Virtual Private Network (VPN) is established between TU/e and TMU in order to implement a reliable and secure data exchange.
- **Socket Configuration.** Data is exchanged between TU/e and TMU as soon as it becomes available using non-blocking Transmission Control Protocol (TCP) sockets running the Internet Protocol (IP). The system's low bandwidth allows for the use of TCP, guaranteeing reliable and orderly data delivery.
- **Data Payload.** The variables exchanged are the following: the current time instant and control signals are sent from the control side to the system side, and the position and orientation measurements are sent from the system side to the controller side.

4.3 Implementation Issues

One of the main implementation issues of the proposed remote tracking controller is the accurate modeling and characterization of the time-delay induced by the communication channel. The use of predictor-like schemes is often discouraged because of their sensitivity to delay model mismatches [5], especially when considering nonlinear systems and a communication channel such as the Internet. To this end, two different methods that ease the implementation of the proposed compensation strategy are suggested. Their objective it to provide an accurate estimate $\tilde{\tau}$ of the real delay τ in practice. The two delay estimation methods studied are explained below:

- **Delay Measurement.** The round trip communication delay between TU/e and TMU (and vice versa) has been measured during different times of the day, for variable amounts of time ranging from $2\,\text{min}$ to $10\,\text{min}$, and for a total time of around $60\,\text{min}$. The mean delay value is approximately $265\,\text{ms}$ for both cases ($267.4917\,\text{ms}$ TU/e→TMU, $269.5307\,\text{ms}$ TMU→TU/e). Occurrences of delays greater than $300\,\text{ms}$ where of 0.27% for TU/e→TMU and 0.34% for TMU→TU/e. Thus, the round trip time-delay is fairly constant and can be modeled with enough accuracy even if the Internet is considered as the communication channel.
- **Signal Bouncing.** The estimator's output may be sent together with the control signals to the mobile robot, and then sent back to the controller without being modified. By using the communication channel itself to delay the estimator's output, modeling the time-delay is no longer necessary (cf. Figure 5).

4.4 Experiments

In the first experiment, a mobile robot at TMU is controlled from TU/e. The reference trajectory is a lemniscate with center at $(0.5\,\text{m}, 0.25\,\text{m})$, a length and width of $0.2\,\text{m}$, and an angular velocity multiplier of $0.2\,\text{m/s}$. The scenario repeats in the second experiment, where a sinusoid with origin at $(0.1\,\text{m}, 0.25\,\text{m})$, an amplitude of $0.15\,\text{m}$, an angular frequency of $0.3\,\text{rad/s}$, and a translational velocity multiplier of $0.01\,\text{m/s}$ constitutes the reference.

The system's initial condition is $q(0) = [0.3235\,\text{m}\ 0.1882\,\text{m}\ 0.2851\,\text{rad}]^T$ for the first experiment and $q(0) = [0.0225\,\text{m}\ 0.1821\,\text{m}\ 0.3916\,\text{rad}]^T$ for the second one. In both cases the estimator's initial condition is set to $z(0) = [0\ 0\ 0]^T$, the controller gains to $c_1 = 1.0$, $c_2 = c_3 = 2.0$ and the correcting term gains to $K_x = K_y = K_\theta = -0.6$. The sampling rate is $25\,\text{Hz}$ and the experiments' duration is $60\,\text{s}$ and $120\,\text{s}$, respectively.

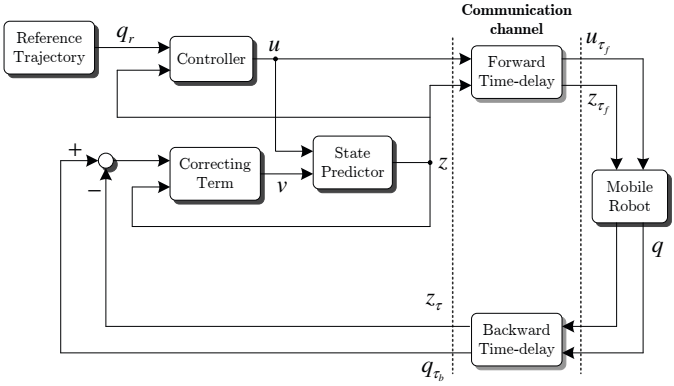

Fig. 5. Remote tracking control strategy block diagram representation using signal bouncing (no time-delay models necessary).

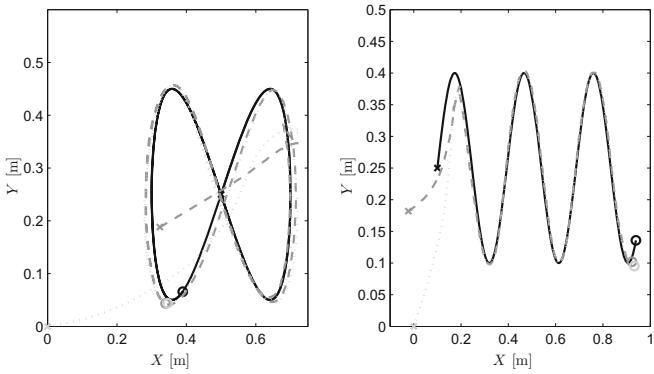

Fig. 6. Reference (black solid line), robot (gray dashed line) and predictor behavior (light gray dotted line) in the X-Y plane for two different trajectories of a robot in Japan controlled from the Netherlands.

The round trip time-delay is modeled as 265 ms based on measurements, although the estimator's output is in fact delayed 280 ms since only delay models which are multiples of 40 ms are allowed due to the setup's sampling time.

The experimental results are shown in Figure 6 and 7 for both experiments. The plots in Figure 6 show the reference (black solid line), robot (gray dashed line) and predictor (light gray dotted line) trajectories in the X-Y plane, with their initial and final position marked with a cross and a circle, respectively. The plots in Figure 7 show the evolution of the error coordinates $z_e(t) = [z_{1_e}(t)\ z_{2_e}(t)\ z_{3_e}(t)]^T$ (black) and $p_e(t) = [p_{1_e}(t)\ p_{2_e}(t)\ p_{3_e}(t)]^T$ (gray) for the first and second experiments (top and bottom, respectively). The error coordinates practically converge to zero even in the presence of a small delay model mismatch and considering a time-varying communication channel. The behavior of the proposed remote tracking controller is consistent with the stability analysis presented and the tracking performance of the robot can be ensured even in the presence of a network-induced delay.

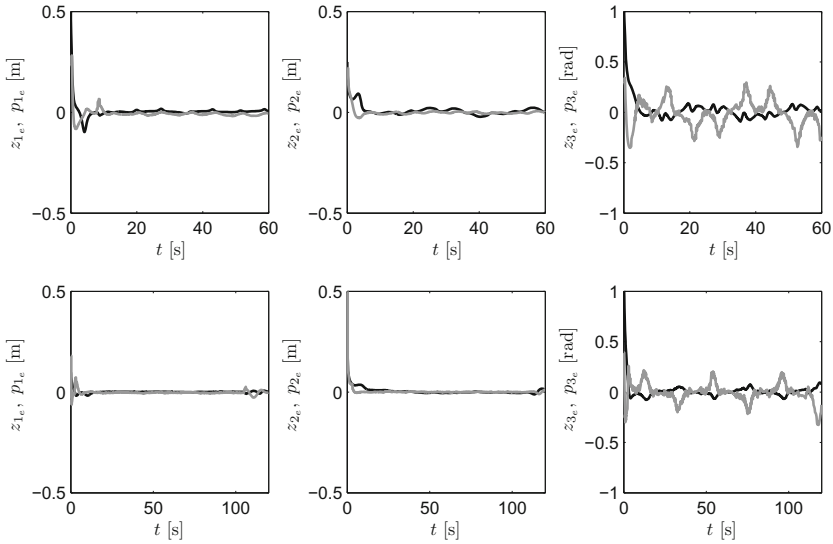

Fig. 7. Practical convergence of the error coordinates $z_e(t)$ (black) and $p_e(t)$ (gray) for the first and second experiments (top and bottom, respectively).

5 Discussion

This paper considers the tracking control problem for a unicycle-type mobile robot controlled over a two-channel communication network which induces time-delays. A tracking control and a state estimator that guarantee tracking a delayed reference trajectory has been proposed. Moreover, a stability analysis showing that the tracking and estimation error dynamics are locally uniformly asymptotically stable has been presented. In addition, experiments validate the effectiveness of the proposed approach and show that the estimator-control strategy can withstand small delay model mismatches and delay variations.

Acknowledgements. The authors are grateful to Prof. Wim Michiels at the Katholieke Universiteit Leuven (KUL) for several useful discussions and communications. This work has been supported by the Mexican Council of Science and Technology (CONACYT), the Mexican Ministry of Education(SEP), the Graduate School of Science and Engineering at TMU, and the Japan Society for the Promotion of Science (JSPS) through Grant-in-Aid for Scientific Research (No. 20560424).

References

1. Brockett, R.: Asymptotic stability and feedback stabilization. In: Differential geometric control theory, pp. 181–191. Birkhäuser, Basel (1983)
2. van den Broek, T.: Formation Control of Unicycle Mobile Robots: Theory and Experiments. Master's thesis, Eindhoven University of Technology (2008)

3. van den Broek, T., van de Wouw, N., Nijmeijer, H.: Formation control of unicycle mobile robots: a virtual structure approach. In: Proceedings of the combined 48th IEEE Conference on Decision and Control and 28th Chinese Control Conference (CDC/CCC), pp. 3264–3269 (2009)
4. Heemels, W.P.M.H., van de Wouw, N.: Stability and stabilization of networked control systems. In: Bemporad, A., Heemels, M., Johansson, M. (eds.) Networked Control Systems. Lecture Notes in Control and Information Sciences, vol. 406, pp. 203–253. Springer, Heidelberg (2010)
5. Hokayem, P.F., Spong, M.W.: Bilateral teleoperation: An historial survey. Automatica 42(12), 2035–2057 (2006)
6. Jakubiak, J., Lefeber, E., Tchón, K., Nijmeijer, H.: Two observer-based tracking algorithms for a unicycle mobile robot. International Journal of Applied Mathematics and Computer Science 12(4), 513–522 (2002)
7. Kanayama, Y., Kimura, Y., Miyazaki, F., Noguchi, T.: A stable tracking control method for an autonomous mobile robot. In: Proceedings of the IEEE International Conference on Robotics and Automation (ICRA), pp. 384–389
8. Kojima, K., Oguchi, T., Alvarez-Aguirre, A., Nijmeijer, H.: Predictor-based tracking control of a mobile robot with time-delays. In: Proceedings of the 8th IFAC Symposium on Nonlinear Control Systems (NOLCOS), pp. 167–172 (2010)
9. Kostic, D., Adinandra, S., Caarls, J., Nijmeijer, H.: Collision-free motion coordination of unicycle multi-agent systems. In: Proceedings of the American Control Conference (ACC), pp. 3186–3191 (2010)
10. Kostic, D., Adinandra, S., Caarls, J., van de Wouw, N., Nijmeijer, H.: Collision-free tracking control of unicycle mobile robots. In: Proceedings of the combined 48th IEEE Conference on Decision and Control and 28th Chinese Control Conference (CDC/CCC), pp. 5667–5672 (2009)
11. Mondada, F., Bonani, M., Raemy, X., Pugh, J., Cianci, C., Klaptocz, A., Magnenat, S., Zufferey, J.C., Floreano, D., Martinoli, A.: The e-puck, a robot designed for education in engineering. In: Proceedings of the 9th Conference on Autonomous Robot Systems and Competitions, pp. 59–65 (2009)
12. Oguchi, T., Nijmeijer, H.: Control of nonlinear systems with time-delay using state prediction based on synchronization. In: Proceedings of the EUROMECH Nonlinear Dynamics Conference (ENOC), pp. 1150–1156 (2005)
13. Oguchi, T., Nijmeijer, H.: Prediction of chaotic behavior. IEEE Trans. on Circuits and Systems I 52(11), 2464–2472 (2005)
14. Oguchi, T., Nijmeijer, H.: Anticipating synchronization of nonlinear systems with uncertainties. In: Proceedings of the 6th IFAC Workschop on Time-Delay Systems (2006)
15. Panteley, E., Lefeber, E., Loría, A., Nijmeijer, H.: Exponential tracking control of a mobile car using a cascaded approach. In: Proceedings of the IFAC Workshop on Motion Control (1998)
16. Python. Python Programming Language (2010), `http://www.python.org`
17. reacTIVision. reacTIVision 1.4: A toolkit for tangible multi-touch surfaces (2010), `http://reactivision.sourceforge.net/`
18. Sedova, N.: Local and semiglobal stabilization in a cascade with delays. Automation and Remote Control 69(6), 968–979 (2008)
19. Tipsuwan, Y., Chow, M.Y.: Control methodologies in networked control systems. Control Engineering Practice 11(10), 1099–1111 (2003)
20. Voss, H.U.: Anticipating chaotic synchronization. Physical Review E 61(15), 5115–5119 (2000)